Speciation in CO₂-loaded aqueous solutions of sixteen triacetoneamine-derivates (EvAs) and elucidation of structure-property relationships

Elmar Kessler^a, Luciana Ninni^a, Tanja Breug-Nissen^a, Benjamin Willy^b, Rolf Schneider^c, Muhammad Irfan^c, Jörn Rolker^b, Werner R. Thiel^d, Erik von Harbou^{a,*}, Hans Hasse^a

Abstract

The speciation in CO₂-loaded aqueous solutions of 16 different derivates of triacetoneamine (EvAs) was investigated in a comprehensive NMR-spectroscopic study. About 350 experiments were carried out for CO₂-loadings up to 3 mole CO₂ per mole amine, temperatures between 20 °C and 100 °C, and a mass fraction of EvA in the unloaded solvent of 0.1 g/g. The observed CO₂-containing species were primary and secondary carbamates, alkylcarbonate, (bi)carbonate, and molecular CO₂. Some EvAs can form zwitterions with a ring structure, which have an important influence on the speciation. From the comprehensive set of data, relationships between the chemical structure of the EvAs and the observed speciation in aqueous solution were established. These results were related to application properties of the EvAs that were taken from previous work. Based on the findings, some general guidelines for the design of new amines were derived and applied for proposing new amines for CO₂-absorption.

Keywords:

 ${\rm CO_2}$ -absorption, derivates of triacetoneamine, structure-property relationships, NMR spectroscopy, speciation of ${\rm CO_2}$ -containing species, zwitterion with a ring structure

Highlights

- Systematic NMR study of the speciation of CO₂-loaded aqueous solutions of 16 amines.
- The amines are all derivates of triacetoneamine with varying substituents.

Email address: erik.vonharbou@mv.uni-kl.de (Erik von Harbou)

^a Laboratory of Engineering Thermodynamics (LTD), University of Kaiserslautern (TUK), P.O. Box 3049, 67653 Kaiserslautern, Germany

^bEvonik Performance Materials GmbH, Rodenbacher Chaussee 4, 63457 Hanau-Wolfgang, Germany
^cEvonik Technology & Infrastructure GmbH, Rodenbacher Chaussee 4, 63457 Hanau-Wolfgang,

Germany

^d Department of Chemistry, University of Kaiserslautern (TUK), P.O. Box 3049, 67653 Kaiserslautern, Germany

^{*}Corresponding author

- Relationships between the chemical structure of the amines and the speciation were elucidated.
- The results were related to application properties.
- Guidelines for the design of new amines were proposed.

1. Introduction

The removal of CO_2 from gaseous streams is an important task, which is often carried out on very large scales [1, 2, 3, 4, 5]. For many applications, the method of choice for the CO₂-removal is reactive absorption with aqueous solutions of amines [6, 7, 8]. The performance of these processes depends crucially on the amine. Understanding the relationship between the chemical structure of the amine and the application properties of the solvent (e.g., CO₂-solubility, rate of absorption of CO₂, enthalpy of absorption of CO₂, and others) is therefore important, especially when the task is to search for new amines with superior performance. Establishing such relationships is a challenge, as they must be based on comprehensive studies that need to be carried out at the same conditions with many different amines to enable a comparison. This has been tried in previous studies [9, 10, 11, 12, 13, 14, 15, 16], but establishing links between the chemical structure of the amine and its properties as lead-component in the solvent has turned out to be difficult on the direct empirical route. We have therefore tried to take a physico-chemical route. The speciation in the reactive solvent plays a key role in this. Figure 1 illustrates the route. In a first step, the relationships between the chemical structure of the amine and the speciation in unloaded and CO_2 -loaded aqueous solutions of amines at relevant conditions are elucidated. In a second step, the information on the speciation is related to the application properties of the solvent that are relevant for the CO₂-absorption process. It is this route which we have followed in the present study.

Determining the speciation of CO_2 -loaded aqueous solutions of amines means quantifying the amounts of protonated/unprotonated amine, bicarbonate and carbonate, carbamates, alkylcarbonates, molecular CO_2 , and eventually other compounds. The state of the art method for determining the speciation of CO_2 -loaded aqueous amine solutions is ¹H and ¹³C NMR spectroscopy [17, 18, 19, 20, 21, 22, 23, 24, 25, 26, 27, 28, 29, 30, 31, 32, 33, 34]. Other spectroscopic methods, such as Infra-red or Raman spectroscopy, have also been applied [35, 36, 37, 38]. Complementary information on the protonated/unprotonated amine can be obtained from measurements of the pK-values of the amines [39, 40, 41, 42, 43, 44, 45, 46] or from measurements of the pH-value in unloaded and CO_2 -loaded aqueous solutions of amines [47, 48].

A particularly interesting class of amines for a systematic study on the speciation in unloaded and CO₂-loaded aqueous solutions of amines are derivates of triacetoneamine, the so-called EvAs, which are known to be promising new solvents for CO_2 -absorption [30, 47, 49, 50]. The EvAs share the triacetoneamine ring structure but differ in one substituent. As many different EvAs have been synthesized for a screening [47], they are ideal candidates to establish structure-property relationships that link information of the chemical structure of the amine with their speciation in aqueous solutions. 21 different EvAs were considered in the present work. Their chemical structures are presented in Figure 2. The amino groups in the EvAs are designated with Greek letters and their pK-values at 40 °C are included in Figure 2. The names of the amines (EvA followed by a number), the designations of the amino groups, and the pK-values were adopted from the previous screening [47], in which also process-relevant application properties were measured for the EvAs. The speciation of CO₂-containing species however had not been studied in the screening. In the present work, for 16 out of the 21 EvAs shown in Figure 2, the speciation of CO_2 -containing species was determined with ^{13}C NMR spectroscopy. The 16 selected EvAs are marked with an asterisk in Figure 2. The remaining EvAs were not investigated as the corresponding variation of the substituent would have added only little information to the study. The speciation was measured in CO_2 -loaded aqueous solutions of EvAs with a mass fraction of EvA in the unloaded solvent of $\tilde{w}_{\text{EvA}}^0 = 0.1 \text{ g/g}$. This concentration was chosen based on previous experience to avoid problems with solid precipitation [47]. CO₂-loading and temperature were varied systematically. All in all, more than 350 NMR experiments were carried out as described in Section 2. The results of this NMR study are presented in Section 3.

The NMR data were combined with results for the pK-values from a previous screening (cf. Figure 2) and relationships between the chemical structure of the amine and the basicity and speciation of CO_2 -containing species were established. This corresponds to the first step of the procedure that is illustrated in Figure 1; its results are presented in the Sections 4.1 and 4.2.

In a second step, the knowledge on the speciation was related to application properties that are relevant for a $\rm CO_2$ -absorption process: $\rm CO_2$ -solubility and rate of absorption of $\rm CO_2$ (c.f. Figure 1). The application property data were taken from the screening [47]. From combining the information from both steps, some guidelines for the design of new amines were derived. Some preliminary results of this procedure have already been described briefly in a conference paper [50], which, however, only contains fragments of the information that is presented here in Section 4.3.

Finally, we have used the guidelines for the design of new amines. Three basic structures as well as several promising derivates of these compounds that can be customized with regard to the requirements of the purification task are proposed in Section 5. Testing these new amines was not in the scope of the present study.

2. Experimental procedure

2.1. Chemicals

The investigated EvAs were provided by Evonik. They were synthesized by reductive amination using a noble metal catalyst [51, 52]. The purity of the EvAs was always \geq 96 mass %. For more details see [47]. CO₂ was purchased from Air Liquide with a purity \geq 99.995 mol %. Ethanol (Uvasol) was purchased from Merck with a purity \geq 99.9 mass %. Potassium bicarbonate was purchased from Sigma Aldrich with a purity \geq 99.5 mass %. The chemicals were used without further purification. H₂O was purified by ion-exchange and filtration with a Siemens TWF/EI-Ion UV Plus water purification system. The resulting purity of H₂O was \geq 99.999 mass %.

2.2. Sample preparation

The aqueous solutions of EvA were prepared gravimetrically, the same way as described in a previous work of our group [30]. The amount of H_2O and EvA were determined with an accuracy of \pm 1 mg. The resulting relative expanded uncertainty of the molality of EvA in aqueous solution \tilde{m}_{EvA} is $U_r(\tilde{m}_{\text{EvA}}) = 0.001$ (0.99 level of confidence).

The aqueous solutions of EvA were loaded with CO_2 by applying a partial pressure of CO_2 of 2 bar onto the gas phase of a stainless steel cylinder which was partially filled with a gravimetrically determined amount of an aqueous solution of EvA. The amount of CO_2 which was added to the cylinder was controlled by the period of time in which the pressure was applied and was determined using NMR spectroscopy as described in Section 2.3. The concentration of CO_2 in the solvent is given as a mole-related CO_2 -loading $\tilde{\alpha}_{CO_2}$, which is defined here as the overall number of moles of CO_2 divided by the overall number of moles of EvA. The mole-related EvA are the molar mass-related EvA and EvA are the molar masses of EvA. In the symbols that are used to describe the composition in the present work, the tilde refers to the overall amounts of the components EvA and EvA and EvA are the molar counting the chemical reactions and their products.

$$\tilde{X}_{\text{CO}_2} = \tilde{\alpha}_{\text{CO}_2} \cdot \frac{M_{\text{CO}_2}}{M_{\text{EvA}}} \tag{1}$$

The designation of the EvAs (EvA followed by a number) are used in the present work not only for designating the amine. For brevity, it is also used for designating aqueous solutions that contain the amine. This short-cut notation is used mainly in the results section and only where the context excludes any confusion with the pure amines.

2.3. NMR spectroscopy

Nuclear magnetic resonance spectroscopy (NMR) was used for the elucidation and quantification of the speciation in the CO₂-loaded aqueous solutions of EvAs. The experimental setup (Bruker Ascend 400 MHz spectrometer equipped with an Avance 3 HD 400 console and either CPPBBO or PABBO 5mm probe heads and Norell S-5-400-MW-IPV-7, Wilmad 522-QPV-7, or Wilmad 524-QPV-7 NMR sample tubes) and procedure was the same as in a previous work of our group [30]. Therefore no details are given here. The mass fraction of EvA in the unloaded solvent was always $\tilde{w}_{\rm EvA}^0 = 0.1 {\rm ~g/g}$.

For the elucidation of the $\rm CO_2$ -containing species, one- and two-dimensional NMR spectroscopic techniques were used (standard $^1\rm H, ^{13}\rm C\{^1\rm H\}$ inverse gated, HMBC, HSQC, and 135° DEPT). The elucidation of the $\rm CO_2$ -containing species was conducted the same way as described in [30].

For the quantification of the CO₂-containing species, 13 C{ 1 H} inverse gated NMR spectra were recorded (decoupling sequence: waltz16, flip angle: 90°, relaxation delay: 90 s, acquired size of FID: 256k, sweep width: 220 ppm, excitation frequency offset: 100 ppm, acquisition time: 6.5 s, and 128 to 1024 scans per spectrum). The T_1 relaxation time was measured by inversion recovery with power gated proton decoupling and was $T_1 \le 8$ s for all studied systems. The recorded spectra were post-processed manually (zero filling, line broadening, phase correction, and either Whittaker-Smoother or polynomial baseline correction). Peak areas were determined by direct integration. The loading of the solution with the CO₂-containing species $\tilde{\alpha}_i$ were conducted by comparing the peak integrals of the different CO₂-containing species i in relation to the total peak integrals of the EvA signals and are thus obtained in moles of the species per moles of all EvA-species in the solution. For simplicity, this loading is called concentration in the present work.

In the symbols that are used to characterize the concentration, the tilde refers to the measured amount of the species and include all protonated forms of the species in the present work. The sum of the concentrations of all CO₂-containing species was taken as the total CO₂-loading as shown in Equation (2). One experiment with each sample was carried out as described above at different temperatures.

$$\tilde{\alpha}_{\text{CO}_2} = \sum_i \tilde{\alpha}_i \tag{2}$$

The standard uncertainty of the measured concentrations of CO_2 -containing species $u(\tilde{\alpha}_i)$ is 5 %, but at least 0.03 mol/mol, between 20 °C and 60 °C and 8 %, but at least 0.05 mol/mol, above 60 °C. For details see [30]. The expanded uncertainty of the molality of EvA is the same as specified in Section 2.2. The expanded uncertainty of the temperature measurement is U(t) = 1 °C (0.99 level of confidence). The pressure inside the NMR tubes was not measured as it has no significant influence on the measured speciation of CO_2 -containing species.

3. Experimental results

3.1. Elucidation of the CO_2 -containing species

Five different types of CO_2 -containing species i were observed in the investigation: primary carbamates, secondary carbamates, alkylcarbonates, (bi)carbonate, and molecular CO_2 . The chemical structure of the five types of CO_2 -containing species are shown in Figure 3. Protonated and unprotonated species cannot be distinguished in NMR spectra. Therefore, in the present work, the given concentrations of CO_2 -containing species include protonated and unprotonated forms. For brevity, carbonate and bicarbonate are lumped together and named (bi)carbonate. Any amino group stabilizes (bi)carbonate. The amino group where the carbamate is formed is given with a Greek letter that corresponds to the amino group labeling of Figure 2.

In the recorded 13 C NMR spectra of the EvAs, the signal of molecular CO_2 can be identified easily, as it is the only signal that appears at about 124 ppm. The signal of molecular CO_2 shows no correlations to any of the $^1\mathrm{H}$ NMR signals in HMBC NMR spectra. The signals of (bi)carbonate, carbamate and alkylcarbonate appear between 155 and 168 ppm. The signal of the carbon atom of (bi)carbonate does not show correlations to any of the proton signals of the EvAs, whereas those of carbamate and alkylcarbonate do. Based on these correlations, the type and position of the carbamate or alkylcarbonate can be assigned unambiguously. Two exemplary elucidations are discussed in detail in the Supporting Information.

None of the investigated EvAs showed carbamate formation at the α -amino group. In contrast, it was found that all EvAs form carbamate at the β -amino group. EvA34 and EvA36 also form carbamate at the γ -amino group. EvA21, EvA27, and EvA31, which contain hydroxy groups, form also alkylcarbonates. No dicarbamates or combinations of a carbamate with an alkylcarbonate at a single EvA were observed in the present work, as they only occur at higher mass fraction of amine and higher CO₂-loadings [30, 24, 34]. (Bi)carbonate was found in all investigated solutions. Molecular CO₂ was observed at high

 CO_2 -loadings for all EvAs except for EvA01, EvA34, and EvA36, where it is probably only observable at higher CO_2 -loadings than the ones investigated in the present work.

3.2. Quantification of the CO_2 -containing species

A set of data for a given EvA usually consists of quantitative NMR results for temperatures between 20 °C and 100 °C in steps of 20 °C and $\rm CO_2$ -loadings up to the one that corresponds to an equilibrium partial pressure of $\rm CO_2$ of about 2 bar at 25 °C. This results in a range of maximal $\rm CO_2$ -loadings of the EvAs between 0.9 mol/mol (EvA32) and 3.1 mol/mol (EvA34). The number of experimental data points was varied between the different EvAs, as it was adapted pragmatically, e.g., accounting for the availability of a given EvA or an occurring liquid-liquid phase separation at elevated temperature.

For a better overview, the 16 EvAs that were investigated here with NMR spectroscopy are divided into six groups. The classification depends on the substituent of the basic triacetoneamine ring structure of the EvAs and is as follows: the substituent contains a primary amino group (Group A), one secondary amino group but no hydroxy group (Group B), at least one hydroxy group (Group C), one secondary amino group and one tertiary amino group (Group D), at least two secondary amino groups (Group E), an ether or carboxylate group (Group F). Although some EvAs fit into more than one group, each EvA was assigned to only one group.

The discussion of the speciation of CO_2 -containing species of the EvAs is done group by group in the following Subsections 3.2.1 to 3.2.6. The results of all NMR experiments are presented in diagrams that show the concentration $\tilde{\alpha}_i$ of the observed CO_2 -containing species carbamates, alkylcarbonates and molecular CO_2 , as a function of the CO_2 -loading, for which numbers for both, \tilde{X}_{CO_2} and $\tilde{\alpha}_{CO_2}$ are shown (cf. Equation (1) and (2)). For clarity, the concentration of (bi)carbonate is not shown in the diagrams but it can be derived from the difference between the CO_2 -loading and the sum of the concentrations of the CO_2 -containing species that are shown. The corresponding numerical experimental data are given in the Supporting Information.

3.2.1. Group A: substituent contains a primary amino group

Group A consists only of EvA01, as this is the only EvA with a primary amino group that was studied here. The observed CO_2 -containing species are β -carbamate and (bi)carbonate. The concentration of β -carbamate is presented in Figure 4. At 20 °C, up to a CO_2 -loading of about 0.3 g/g, more CO_2 is chemically bound as β -carbamate than as (bi)carbonate. At higher CO_2 -loading, (bi)carbonate dominates. The concentration of β -carbamate as a function of the CO_2 -loading shows a maximum, which is 0.7 mol/mol

at 20 °C. With increasing temperature, the maximum decreases and shifts towards lower $\rm CO_2$ -loadings.

3.2.2. Group B: substituent contains one secondary amino group

EvA02, EvA04, and EvA05 form Group B in which the substituents are alkane amines with one secondary amino group. The observed CO_2 -containing species are β -carbamate, (bi)carbonate, and molecular CO_2 . The concentration of β -carbamate and molecular CO_2 of the three EvAs are shown in Figure 5. They form very low concentrations of β -carbamate, which are all below about 0.03 mol/mol. Almost all CO_2 is chemically bound as (bi)carbonate. With increasing temperature, the concentration of β -carbamate decreases. Small amounts of molecular CO_2 are observed at high CO_2 -loading. The concentration of molecular CO_2 increases with increasing temperature.

3.2.3. Group C: substituent contains at least one hydroxy group

EvA21, EvA27, and EvA31 form Group C in which the substituents contain at least one hydroxy group. The observed CO_2 -containing species are β -carbamate, alkylcarbonate, (bi)carbonate, and molecular CO_2 . The concentration of β -carbamate, alkylcarbonate, and molecular CO_2 of the three EvAs are shown in Figure 6. The concentration of β -carbamate as a function of the CO_2 -loading shows a maximum while the concentration of alkylcarbonate continuously increases. For EvA21, the concentration of β -carbamate and alkylcarbonate are similar whereas for EvA27 and EvA31, the concentration of β -carbamate is higher than that of alkylcarbonate. Molecular CO_2 was observed at high CO_2 -loadings for all three EvAs. The concentration of β -carbamate and alkylcarbonate decreases with increasing temperature, that of molecular CO_2 increases.

3.2.4. Group D: substituent contains one secondary and one tertiary amino group

EvA03, EvA07, EvA24, EvA25, and EvA26 form Group D, in which the substituents contain one secondary amino group and one tertiary amino group. The observed CO₂-containing species are β -carbamate, (bi)carbonate, and molecular CO₂. The concentration of β -carbamate and molecular CO₂ of the five EvAs are shown in Figure 7. For EvA03 and EvA25, the concentration of β -carbamate as a function of the CO₂-loading shows a maximum, which are 0.2 mol/mol for EvA03 and 0.22 mol/mol for EvA25. For EvA07, EvA24, and EvA26 the concentration of β -carbamate continuously increases with increasing CO₂-loading. The maximum concentration of β -carbamate was 0.3 mol/mol for EvA07, 0.06 mol/mol for EvA24, and 0.53 mol/mol for EvA26. Molecular CO₂ was observed at high CO₂-loadings, for all EvAs of this group. The concentration of β -carbamate decreases with increasing temperature, that of molecular CO₂ increases.

3.2.5. Group E: substituent contains at least two secondary amino groups

EvA34 and EvA36 form Group E, in which the substituents contain at least two secondary amino groups. The observed CO₂-containing species are β -carbamate, γ -carbamate, and (bi)carbonate. The concentration of β -carbamate and γ -carbamate of the two EvAs are shown in Figure 8. The concentration of γ -carbamate of EvA34 is up to 0.83 mol/mol at 20 °C. This is the highest carbamate concentration of all EvAs in the investigation. The concentration of γ -carbamate increases with increasing CO₂-loading until it reaches a maximum where the concentration does not change significantly upon a further increase of the CO₂-loading. Only small amounts of β -carbamate of around 0.07 mol/mol are observed for EvA34. For EvA36, the concentration of β -carbamate and γ -carbamate show a maximum as a function of the CO₂-loading, which is 0.46 mol/mol for γ -carbamate and 0.15 mol/mol for β -carbamate at 20 °C. The maximum of γ -carbamate is found at lower CO₂-loadings than that of β -carbamate. For both EvAs of Group E, the concentration of β -carbamate and γ -carbamate decreases with increasing temperature.

3.2.6. Group F: substituent contains an ether group or a carboxylate group

EvA06 and EvA32 form Group F. The substituent of EvA06 contains an ether group, that of EvA32 an carboxylate group. The observed CO_2 -containing species are β -carbamate, (bi)carbonate, and molecular CO_2 . The concentration of β -carbamate and molecular CO_2 of the two EvAs are shown in Figure 9. Both EvAs show particularly high concentrations of molecular CO_2 . The maximal concentration of molecular CO_2 for EvA06 was 0.25 mol/mol at 80 °C, which was the highest concentration of molecular CO_2 of all studied EvAs. The maximal concentration of molecular CO_2 for EvA32 was 0.13 mol/mol and was found at 60 °C. For both EvAs, the concentration of β -carbamate as a function of the CO_2 -loading shows a maximum at 20 °C, which is about 0.07 mol/mol for EvA06 and 0.03 mol/mol for EvA32. With increasing temperature, the concentration of β -carbamate decreases and that of molecular CO_2 increases. The maximum CO_2 -loading of EvA32 which was obtained due to the loading process (cf. Section 2.2) was the lowest of all EvAs. It was below 1 mol/mol.

4. Structure-property relationships

In this section, the structure-property relationships are presented according to the route that we have followed in the present work (cf. Figure 1). The first step of the route was to establish relationships between the chemical structure of the EvAs and their basicity as well as between the chemical structure of the EvAs and their speciation of $\rm CO_2$ -containing species. These relationships are presented in the Sections 4.1 and 4.2 and

base on the pK-values which were measured in the previously performed screening [47] and the results from NMR measurements of the present work.

The second step of the route was to link the established relationships from Section 4.1 and 4.2 with application properties of the solvent, which are relevant for a CO₂-absorption process, e.g., data on the rate of absorption of CO₂ and equilibrium CO₂-loading which are available from the screening [47]. From these links, guidelines for the design of new amines were derived. This second step is presented in Section 4.3.

Some of the relationships lead to counteracting trends. This has to be taken into account when trying to verify a given relationship by comparing different amines. Each relationship is introduced in the following using results for an EvA in which the effect described by the relationship is dominant.

4.1. Basicity: pK-value and BM-value

pK-values are valuable indicators for a comparison of the basicity of single amino groups. However, for a quantitative comparison of the basicity of amines, especially if the amines have different number of amino groups, the pK-values are insufficient. Therefore, a dimensionless number that enables a quantitative comparison of the basicity of the EvAs, independent of the number of amino groups in the EvAs, was introduced in a previous work of our group [50]. The dimensionless number is named BM-value (BM stands for basicity per mass) and is calculated from Equation (3) by dividing the sum of all pK-values of a given EvA p K_{EvA} by the molar mass of the EvA M_{EvA} . The BM-value at 40 °C of the investigated EvAs are given in Table 1. Both, the BM-value and the pK-values are considered in the following discussion.

$$BM = \frac{\sum pK_{\text{EvA}}}{M_{\text{EvA}}} \cdot 100 \tag{3}$$

- 1) The addition of oxygen atoms to the substituents of the EvAs (EvA06, EvA09, EvA21, EvA24, EvA27, EvA31, EvA32) lowers the pK-values of the amino groups (cf. Figure 2). This has already been reported for the EvAs [47] and was found for other classes of amines as well [24, 39, 40, 41, 42]. The decrease of the pK-values is caused by the positive inductive effect of oxygen atoms. Further, the oxygen atoms add molar mass to the EvAs which, in combination with the lowered pK-values, lowers the BM-value (cf. Table 1). This leads to the fact that the seven oxygen-containing EvAs are among the nine EvAs with the lowest BM-value in the comparison.
- 2) EvA19 contains a furane ring (cf. Figure 2). The aromatic structure lowers the basicity and increases the molar mass such that EvA19 has one of the lowest BM-values in the study (cf. Table 1). Similar results for other amines that contain aromatic ring structures were reported in literature [11].

- 3) In contrast to expectations, the negative inductive effect of the carboxylate group of EvA32 does not show an exceptional influence on the pK-value of the β -amino group (cf. Figure 2). However, the oxygen atoms and the potassium atom add much molar mass such that the BM-value of EvA32 is one of the lowest in the study (cf. Table 1).
- 4) By replacing an ethyl group between the β and the γ -amino group (EvA07 and EvA26) with a propyl group (EvA03 and EvA25), the pK-values of both amino groups and the BM-value increases (cf. Figure 2 and Table 1). A decrease of the BM-value as a result of the increasing molar mass due to the addition of one CH₂ group is overcompensated by an increase in the pK-values of the β and the γ -amino group, resulting from the positive inductive effect of the added group. n-Butyl groups may also lead to higher BM-values [53] but were not investigated in this study.
- 5) The substitution of two methyl groups at the γ -amino group (EvA03 and EvA07) by two ethyl groups (EvA25 and EvA26) increases the pK-values of the γ -amino groups (cf. Figure 2), but lowers the BM-value (cf. Table 1). The increase of molar mass by the two added carbon atoms exceeds their positive inductive effect. A combination of a methyl and an ethyl group might lead to higher BM-values compared to two methyl groups but was not investigated in this study.
- 6) The addition of one methyl group at the end of the alkyl chain of isopropylamine (EvA04) to sec-butyl amine (EvA05) does not have a significant influence on the pK-value of the β -amino group (cf. Figure 2), but lowers the BM-value as a result of the increased molar mass (cf. Table 1). Alkyl chains of terminating ligands with less than three carbon atoms might further increase the BM-value but were not investigated in this study.
- 7) Tertiary amino groups in ring structures have much lower pK-values than tertiary amino groups in chains. The same trend can be found by comparing pK-values of other amines than the EvAs [40, 42]. A good example for this effect is given by the comparison of the pK-values of the γ -amino groups of EvA24 and EvA21 (cf. Figure 2). Despite the larger positive inductive effect of the morpholine group of EvA24, compared to that of the two ethanol groups of EvA21, the pK-value of the γ -amino group of EvA24 is significantly lower than that of EvA21. A further example is the lower pK-value of the γ -amino group of EvA14 compared to that of EvA03, which is also contrary to the expected inductive effect of the surrounding alkyl groups. It is conceivable that the higher rigidity of a ring structure compared to that of a chain-structure causes the observed differences in the pK-values.
- 8) The pK-values of secondary amino groups are higher than those of similar tertiary amino groups. This is well-known in literature [40, 41, 54]. An example from the present work is given by the comparison of the pK-values of the γ -amino group of EvA36 and

EvA03 (cf. Figure 2). Despite the higher positive inductive effect of two methyl groups on the γ -amino group of EvA03, compared to that of one methyl group for EvA36, the pK-value of the γ -amino group of EvA03 is lower than that of EvA36. Also the BM-value increases as the removal of one methyl group reduces the molar mass while simultaneously the pK-value of the amino group increases. The effect is enhanced if the tertiary amino group is part of a ring structure (cf. EvA06 compared to EvA09 in Figure 2). The reason for this observation is probably the better spatial accessibility of the free electron pair of secondary amino groups, compared to that of tertiary amino groups. The better spatial accessibility predominates the stronger positive inductive effect of a third alkyl group.

4.2. Speciation of CO_2 -containing species

4.2.1. Formation of ring structures

The results of the present work and of a previous work of our group [50] indicate that carbamates and alkylcarbonates are stabilized by the formation of H-bond and zwitterionic stabilized ring structures. Even though no direct evidence for the existence of such ring structure was found, the obtained results strongly indicate that they can be formed. By postulating their existence, simple and plausible explanations for the observed results can be given that would otherwise be contradictory, namely regarding the carbamate and alkylcarbonate formation.

Ring formations in aqueous solutions of amines have been postulated previously; mainly between hydroxy- and amino groups [9, 45, 55, 56, 57], but also between carbamates and amino groups [18, 50]. However, to the best of our knowledge, the present work is the first in which a systematic experimental study gives not only indications for the existence of such H-bond and zwitterionic stabilized ring structures, but also provides information on the conditions, under which they are formed and the consequences they have on the properties of the aqueous solvent.

Carbamate and amino group

The formation of a zwitterion with a ring structure between a carbamate and an amino group is schematically shown in Figure 10, using EvA07 as an example. For clarity, the reaction scheme focuses only on the steps which are directly relevant for the formation of the zwitterion. Other information such as that on protonation states of the amino groups that are not involved is not included. The reaction scheme starts with the components EvA07, H_2O , and CO_2 on the left side. R_I is the protonation of the β -amino group as well as the formation of bicarbonate. R_{II} is the formation of β -carbamate and R_{III} is the conversion between the CO_2 -containing species bicarbonate and carbamate. These reactions are basically known [58]. R_{IV} is the formation of the carbamate zwitterion. This

step has, to the best of our knowledge not been described before in the literature, and is assumed to exist not only for EvAs but also for other amines. The protonated positively charged γ -amino group orients itself towards the negatively charged oxygen atom of the β -carbamate and forms a zwitterion with a stabilizing ring structure. The ring structure is stabilized by ionic and H-bond interactions between the amino group and the carbamate. Due to the stabilizing effect, larger concentrations of carbamate were found for EvAs that form a zwitterion with a ring structure. This is illustrated by the comparison of the concentrations of β -carbamate of EvA02 (cf. Figure 5) with those of EvA03, EvA07, EvA24, EvA25, and EvA26 (cf. Figure 7). EvA02 can only form a zwitterion with the α -amino group of the boat-conformation of the 2,2,6,6,Tetramethylpiperidine ring. This confirmation is unstable and thus plays a minor roll in this study. The resulting concentration of β -carbamate of EvA02 is low. The other amines can form a zwitterion also with the γ -amino group. This ring structure is much more stable, which results in much higher concentrations of β -carbamate. The differences between the concentrations of β -carbamate of the EvAs that form the stable zwitterion result from the different stability of the zwitterions. Two parameters that influence the stability of the zwitterions were found in the study.

1) A high pK-value of the amino group that is involved in the zwitterionic structure enhances the stability of the carbamate zwitterion. For instance, this can be seen from the results for EvA07 and EvA26 shown in Figure 7. Both EvAs form a seven-membered zwitterionic stabilized ring (counting the carbon (#1) and the negatively charged oxygen atom of the β -carbamate (#2), the β -amino group (#3), the two carbons between the β and γ -amino group (#4, #5), the γ -amino group (#6) and the proton that is attached to the protonated γ -amino group (#7)). The basicity of the γ -amino group of EvA26 is higher than that of the γ -amino group of EvA07 (cf. Figure 2). This results in a higher concentration of β -carbamate for EvA26 than for EvA07. The same trend is observable for EvA03, EvA24, and EvA25. EvA03, EvA24, and EvA25 form eightmembered zwitterionic stabilized rings (counting the carbon (#1) and the negatively charged oxygen atom of the β -carbamate (#2), the β -amino group (#3), the three carbons between the β - and γ -amino group (#4, #5, #6), the γ -amino group (#7) and the proton that is attached to the protonated γ -amino group (#8)). The concentration of β -carbamate of these EvAs decreases with decreasing pK-value of the γ -amino group. It can be assumed that the higher pK-values of the γ -amino group leads to a higher concentration of the protonated species, which consequently leads to higher concentrations of stabilized β -carbamate.

2) Zwitterions with seven-membered rings are more stable than zwitterions with eight-membered rings. This can be seen from the results for EvA25 and EvA26 shown in Figure 7. Even though the pK-value of the γ -amino group of EvA25 is higher than that of EvA26 (cf. Figure 2), the concentration of γ -carbamate of EvA25 is lower than that of EvA26. The same trend is found for EvA03 and EvA07 (cf. Figure 7).

Carbamate and hydroxy group

The β -carbamate of the hydroxy group containing EvA27 and EvA31 (cf. Figure 6) are stabilized by H-bond interaction with the proton of their respective hydroxy group. This stabilizing interaction between carbamate and hydroxy group is schematically shown in the left part of Figure 11 and resembles the carbamate zwitterion shown in Figure 10. The stabilizing effect can be seen from a comparison of the results of EvA31 (cf. Figure 6), with the results of EvA02 and EvA06 (cf. Figure 5 and Figure 9) as well as with EvA03, EvA07, EvA25, and EvA26 (cf. Figure 7). The concentration of the H-bond stabilized β -carbamate of EvA31 is significantly higher than that of EvA06 and EvA02, which are not stabilized. However, it is also lower than that of EvA03, EvA07, EvA25, and EvA26, which are stabilized by a zwitterion. This indicates that the stabilizing effect of the H-bond is weaker than that of the zwitterion, but strong enough to increase the concentration of β -carbamate compared to the EvAs with no stabilizing effect.

Alkylcarbonate and amino group

Alkylcarbonates are formed between CO₂ and hydroxy groups at alkaline conditions. Accordingly, alkylcarbonates were found for EvA21, EvA27, and EvA31. The alkylcarbonates of EvA21, EvA27, and EvA31 are additionally stabilized by a zwitterion with a ring structure that is formed between the negatively charged alkylcarbonate and the positively charged β -amino group for EvA27 and EvA31 and the γ -amino group for EvA21, respectively. Such an alkylcarbonate zwitterion is schematically shown in the right part of Figure 11. Same as the carbamate zwitterion, it is stabilized by ionic and H-bond interactions. EvA21 shows a significantly higher concentration of alkylcarbonate than EvA27 and EvA31. This is probably due to the higher basicity of the interacting γ amino group of EvA21 compared to that of the β -amino group of EvA27 and EvA31. It can be assumed that the alkylcarbonate species, that were found in CO₂-loaded aqueous solutions of mono-ethanolamine and methyl-diethanolamine (MDEA) in previous works of our group [33, 34] are also stabilized by the formation of zwitterions with a ring structure. A study of CO₂-loaded aqueous solutions of ethanol proved that alkylcarbonates are formed also without being stabilized in a ring structure, as long as the CO₂-loaded aqueous solution is at alkaline conditions. For more details see Supporting Information.

4.2.2. Steric hindrance

The substituents of carbon atoms that are adjacent to primary and secondary amino groups have a strong influence on the speciation of CO_2 -containing species. This influence is often labeled as steric effect or steric hindrance. In the discussion of the present work, we refer to different degrees of steric hindrance that are defined according to Figure 12. The degree depends on the number of hydrogen atoms (H) that are covalently bound to carbon atoms which are adjacent to the amino group (R, R_l, R_r in Figure 12). A distinction of the hindrance is made between unhindered, single-hindered, double-hindered, triple-hindered, and quadruple-hindered amino groups (cf. Figure 12). In the following section, the influence of the differently hindered amino groups on the speciation of CO_2 -containing species is discussed.

- 1) Unhindered and single-hindered primary amino groups show high concentrations of carbamate [18, 22, 28, 59]. EvA01 is the only amine in this study that contains a primary amino group (cf. Figure 2). The β -amino group of EvA01 is single-hindered and shows high concentrations of β -carbamate (cf. Figure 4). The good spatial accessibility of unhindered and single-hindered primary amino groups promotes the formation of carbamate.
- 2) Unhindered secondary amino groups show high concentrations of carbamate [18, 22, 28, 60]. In the present work, EvA34 and EvA36 were the only EvAs that contain an unhindered secondary amino group (cf. Figure 2). Both EvAs show high concentrations of γ -carbamate at the unhindered secondary γ -amino group (cf. Figure 8). However, this γ -carbamate formation is additionally promoted by the formation of a zwitterion with a ring structure.
- 3) Increased steric hindrance lowers the stability of zwitterionic stabilized ring structures between carbamates and protonated amino groups. This is demonstrated by the concentration of EvA36 which forms two carbamate species that are stabilized by the formation of eight-membered carbamate zitterion rings: β -carbamate and γ -carbamate (cf. Figure 8). β -carbamate is formed at the single-hindered secondary β -amino group and is stabilized by the γ -amino group which has a high pK-value, whereas γ -carbamate is formed at the unhindered secondary γ -amino group and is stabilized by the β -amino group, which has a lower pK-value. Regarding only the basicity, the concentration of β -carbamate should exceed the concentration of γ -carbamate due to the more stable zwitterionic ring structure. However, the observed concentrations show the opposite trend (cf. Figure 8), which can be interpreted as a result of the increased hindrance of the β -amino group compared to that of the γ -amino group. For EvA34 the influences of the steric hindrance and that of the basicity on the zwitterions are superimposed (cf. Figure 8).

The γ -carbamate of EvA34 is less hindered than the β -carbamate and additionally forms a strong zwitterion with the δ -amino group. Therefore, the concentration of γ -carbamate of EvA34 exceeds that of the β -carbamate by far.

- 4) Increased steric hindrance of hydroxy groups lowers the stability of alkylcarbonate zwitterions and H-bond interaction stabilized carbamates in which the hydroxy group is involved. By applying the same definition of steric hindrance of primary amines from Figure 12 to hydroxy groups, the hydroxy group of EvA27 is defined as single-hindered, and the hydroxy group of EvA31 is defined as unhindered (cf. Figure 2). The concentration of β -carbamate and alkylcarbonate of the unhindered EvA31 exceeds the respective concentrations of the single-hindered EvA27 (cf. Figure 6). As the basicity and ring-size are similar, this is most likely caused by the hindrance of the interacting hydroxy group.
- 5) Single and double-hindered amino groups only show very low concentrations of carbamate if the carbamate is not stabilized by a zwitterion with a ring structure. This can be seen from the concentration of β -carbamate of EvA02 (cf. Figure 5), which is single-hindered, and EvA04 and EvA05 (cf. Figure 5), which are double-hindered and which all three are not stabilized. A difference between single-hindered and double-hindered secondary amino groups concerning the concentration of β -carbamate was not found in the study. If the carbamate at single hindered secondary amino groups is stabilized by a zwitterion with a ring structure however, high concentrations of carbamate are observable (cf. Figure 7).
- 6) For none of the EvAs a formation of carbamate at the quadruple-hindered secondary α -amino group was observed. Even though no triple-hindered secondary amino groups were investigated in the present work, it can be assumed that also triple-hindered secondary amino groups do not form significant amounts of carbamate.
- 7) Steric hindrance influences the amount of (bi)carbonate that can be captured in the aqueous solution of EvA. EvA02 and EvA05 have the same molar mass and similar pK-values of all amino groups, but they differ in the hindrance of the β -amino group, which is single-hindered for EvA02 and double-hindered for EvA05 (cf. Figure 2). Even though they also have a similar speciation of CO₂-containing species, i.e. CO₂ is mainly bound as (bi)carbonate (cf. Figure 5), they reveal strong differences in the equilibrium CO₂-loadings at low temperature. This is shown in Table 2 where the equilibrium CO₂-loading \tilde{X}_{CO_2} of EvA02 and EvA05 at three different conditions (C1 to C3) are given. The conditions vary in the temperature t, in the mass fraction of EvA in the unloaded solvent \tilde{w}_{EvA}^0 , and in the equilibrium partial pressure of CO₂ p_{CO_2} . At low temperature (C1 and C2 in Table 2), the equilibrium CO₂-loading of EvA02 is much higher than that of EvA05. As almost all CO₂ is bound as (bi)carbonate, this means that single-hindered

secondary amino groups enhance the solubility of (bi)carbonate in the solvent, compared to double-hindered amino groups. It can be assumed that the better accessibility of less hindered amino groups promotes a short-range coordination between (bi)carbonate and the amino group which stabilizes the (bi)carbonate. This effect was not observed at high temperature (cf. C3 in Table 2).

4.2.3. Ether groups

Ether groups enhance the solubility of molecular CO_2 ; therefore physical solvents for CO_2 -absorption often contain ether groups [1, 61]. This is in line with the findings for the ether group containing $\mathrm{EvA06}$, for which the highest concentrations of molecular CO_2 in the present study were found (cf. Figure 9). For $\mathrm{EvA24}$ in contrast, where the oxygen atom is placed in a ring, the concentration of molecular CO_2 is low (cf. Figure 7). This unexpected low concentration of molecular CO_2 in the aqueous solutions of $\mathrm{EvA24}$ is probably due to a superposition with other effects, like the differing basicity, the formation zwitterions with a ring structure, or the less flexible placement of the oxygen atom inside a ring structure.

The concentration of β -carbamate of the ether group containing EvA06 (cf. Figure 9) is higher than that of EvA02 (cf. Figure 5). A reason for this may be the lower pK-value of the β -amino group of EvA06 compared to that of EvA02 (cf. Figure 2). Low pK-values are suspected to favor the formation of carbamate [62, 63]. However, the influence of the ether group or the high concentration of molecular CO₂ on the concentration of β -carbamate are superimposed for EvA06, which complicates a final explanation of the observed higher concentration of β -carbamate.

4.3. Application properties

In this section, the relationships between the chemical structure of the EvAs and the speciation of CO₂-containing species and basicity, which were established in Section 4.1 and 4.2, are related to application properties of the solvents that are directly relevant for the CO₂-absorption process. This includes quantitative relationships to measured data for the equilibrium CO₂-loading and rate of absorption of CO₂, which were established in the screening [47], as well as general considerations regarding the mass transfer, solubility and volatility of the amine, and energy demand of a given absorption/desorption process.

Figure 13 a) shows the equilibrium CO_2 -loading \tilde{X}_{CO_2} of aqueous solutions of EvAs at 40 °C and 100 °C and Figure 13 b) the initial rate of absorption of CO_2 RA at 40 °C as a function of the BM-value (cf. Section 4.1), respectively. Both, equilibrium CO_2 -loading and rate of absorption of CO_2 were measured at a mass fraction of EvA in the unloaded solvent of $\tilde{w}_{EvA}^0 = 0.05$ g/g and a partial pressure of CO_2 of $p_{CO_2} = 140$ mbar [47].

In average, the equilibrium CO_2 -loading increases with increasing BM-value. This is observable for both temperatures. The slope however differs between the two temperatures, which leads to an average increase of the difference between the equilibrium CO_2 -loadings at the two temperatures with increasing BM-value. Also the rate of absorption of CO_2 increases with increasing BM-value. The equilibrium CO_2 -loading can be seen as the driving force for the absorption which is why the rate of absorption of CO₂ correlates with the equilibrium CO_2 -loading [47] and hence, also with the BM-value. For the absorption of CO₂, high CO₂-loading and high rate of absorption of CO₂ at 40 °C are desired. For the desorption, a low energy demand for the regeneration of the solvent is preferred, for which to achieve a large difference between the equilibrium CO₂-loadings at 40 °C and 100 °C, low equilibrium CO₂-loading at 100 °C, and low enthalpy of absorption of CO₂ contribute in varying degrees, depending on the purification task that is performed [47]. The enthalpy of absorption of CO_2 is strongly influenced by the speciation. Broadly generalized, it is small for solvents where CO₂ is captured as molecular CO₂, medium for solvents that mainly form (bi)carbonate and high for solvents where significant concentrations of carbamate are formed [1, 7, 26, 64, 65, 66, 67].

As expected, amines that contain carboxylate groups show low equilibrium CO_2 -loadings, low differences between the equilibrium CO_2 -loadings, and low rates of absorption of CO_2 and should be avoided in the design of good performing amines. The same was found for aromatic structures [11, 29, 47, 68, 69].

Oxygen atoms have a negative effect on the BM-value which is rather undesired regarding equilibrium CO_2 -loading and rate of absorption of CO_2 (cf. Figure 13). Oxygen atoms that are part of a ring structure should generally be avoided. ether groups which are not part of a ring structure however significantly improve the solubility of molecular CO_2 in the solvent. This usually lowers the energy demand for the regeneration of the solvent and is advantageous in purification tasks where properties of a physical solvent are wanted, e.g., in tasks where the partial pressure of CO_2 in the feed gas is high and the purification requirement is low.

The addition of hydroxy groups significantly increases the water-solubility and decreases the volatility of the amine [46, 70]. Due to the lower volatility, the molecule size of the amine can be reduced which lowers the dynamic viscosity and enhances the mass transfer of CO_2 . Additionally, hydroxy groups form alkylcarbonates which is an additional reaction pathway for the absorption of CO_2 that should increases the rate of reaction of CO_2 compared to similar systems without that reaction [71]. If high mass transfer and low volatility is absolutely essential in the purification task, the addition of hydroxy groups may be considered. Otherwise hydroxy groups should be avoided and

di- or triamines should be favored as they lower the volatility due to their molar mass without generating disadvantageous ratios between alkyl and amino groups. The optimal distance between two amino groups is three to four carbon atoms. A ring structure between the amino groups is advantageous as its steric influence impedes the formation of zwitterions which reduces the equilibrium CO_2 -loadings and probably also the enthalpy of absorption of CO_2 . The length of terminating alkyl ligands of secondary amino groups should have not more than three carbon atoms.

Tertiary amino groups that are part of a ring structure should be avoided due to their low BM-value compared to tertiary amino groups that are not part of a ring structure, resulting in low equilibrium CO_2 -loading and low rate of absorption of CO_2 . Secondary amino groups should be preferred over tertiary amino groups due to the increased BM-value and enabled reaction pathway of the formation of carbamate, from which the equilibrium CO_2 -loading and the rate of absorption of CO_2 benefits.

Unhindered secondary amino groups form stable carbamates. Stable carbamates increase the CO_2 -solubility at low partial pressure of CO_2 [7, 30, 47, 60], which is advantageous if the requirement for the residual amount of CO_2 in the purified gas stream is very low, but increase the energy demand for the regeneration of the solvent. Single-hindered secondary amino groups show stable carbamates only if the carbamate is stabilized by a zwitterion with a ring structure. By avoiding the stabilization, the carbamate constitutes as an intermediate (cf. Figure 10), which we believe is advantageous for the rate of reaction of CO_2 , the amount of CO_2 that can be captured, and the energy demand for the regeneration of the solvent. A higher degree of steric hindrance than single hindered is disadvantageous as it reduces the amount of bi(carbonate) that is captured.

From the investigated amino groups, single-hindered secondary amino groups emerge as advantageous in many aspects and seem to be especially favorable to reduce the energy demand for the regeneration without showing obvious deficiencies in other properties, e.g., the rate of absorption of CO_2 . Also other amines that contain a single hindered secondary amino group were evaluated positively in literature [11, 16, 22, 24, 57].

5. Design of new amines

In this section, the structure-property relationships from Section 4 are used for the design of new amines. This is a backward run through the steps that were taken to elucidate the structure-property relationships (cf. Figure 1), which means that desired application properties are selected and the corresponding optimized chemical structure is designed. Thereby, different purification tasks lead to different chemical structures. There is no single best design for all purification requirements. Nevertheless, some general rules

can be applied for the design of basic structures which can then be tailored to fit best for a given purification task.

Three of such basic structures are proposed in the presend work. These amines are abbreviated by the acronym ADAM which stands for Advanced Designed Amines with a consecutive capital letter, designating the structure. The chemical structure of the ADAMs are shown in the upper part of Figure 14. Intermediates that can be used as starting materials for the synthesis of the proposed ADAMs are commercially available (CAS No.: 71322-99-1, 1245698-19-4, 59663-72-8, 183591-49-3, 3114-70-3, 637-88-7, 3385-21-5, 504-02-9) and routes for the synthesis of the ADAMs are known [52]. All ADAMs contain two amino groups which slightly differ in their position.

In the ADAMs that are shown in the upper part of Figure 14, R₁ and R₂ mark the positions where modifications are intended, and by which the application properties of the molecules can be adjusted to the requirements of the purification task. To lower the energy demand, R₁ and R₂ may be methyl, ethyl, or propyl groups, as well as dimethyl-, ethyl methyl-, diethyl-, propyl methyl-, propyl ethyl-, or n-butyl methyl-ethers. To increase the CO₂-solubility at low partial pressure of CO₂, R₁ and/or R₂ may be a proton so that the ADAMs contain primary and/or unhindered secondary amino groups. To lower the volatility of the ADAMs, the substituents which are shown in the lower part of Figure 14 may be added at R₂. They were also designed based on the structureproperty relationships of this work. The substituents or at least intermediates of them are commercially available (CAS No.: 42042-71-7, 110-60-1, 78-93-3, 107-87-9, 278789-37-0, 1550959-11-9, 1785070-11-2, 1236121-42-8, 2167461-04-1) and the routes for their synthesis and addition to the ADAMs are known [52]. R₃ is intended for further modifications. Due to the already high molar mass, only methyl or ethyl groups should be considered as substituents here. In case that the ADAMs are insufficiently soluble in water or show too high volatility, methanol, ethanol, propanol or n-butanol groups could also be considered for the positions R_1 or R_2 .

6. Conclusions

The speciation of CO_2 -containing species in 16 aqueous solutions of EvAs was measured between 20 °C and 100 °C in the present work using NMR spectroscopy. The observed CO_2 -containing species were carbamates of primary and secondary amino groups, alkylcarbonates, (bi)carbonate, and molecular CO_2 . The data on the speciation were combined with data on the pK-values of the EvAs and relationships between their chemical structure and the observed speciation and basicity were established. Many of the results, that were obtained here for the EvAs can be generalized and applied to other

amines. Some relationships, that had been described previously in literature for other amines were confirmed. Others were stated in the present work for the first time. Regarding these new relationships, some conclusions made in literature need to be reconsidered, e.g., in [12, 18, 25, 44, 45].

The established relationships were summarized and compared to application properties of the solvents, which are relevant for a CO₂-absorption process. From this comparison, some general guidelines for the design of new amines were derived. These guidelines were applied and three new basic chemical structures, called ADAMs, as well as a selection of substituents for the ADAMs were proposed. The ADAMs and their derivates provide a modular kit for the design of tailor-made amines for a variety of purification tasks for which, dependent on the substituent, the application properties of the amine can be adapted to the requirements of the purification task. The new amines can be synthesized from intermediates which are commercially available.

The next step on the pathway towards tailor-made amines would be to synthesize some ADAMs and investigate them in a thorough manner as it was done for the EvAs. This will show if they meet the expectations, drawn from the relationships of the present work. Furthermore, there are still many influencing parameters which are unknown and which need to be studied, e.g., the effect chemical groups which were not part of the present work, or the influence of interactions between functional groups which are not part of the same molecule [19, 28], which may lead to more new chemical structures or substituents of the ADAMs. If the ADAMs meet the expectations, still the complexity of their synthesis, the price of the molecules, their thermal and chemical stability, toxicity as well as further physico-chemical properties namely the dynamic viscosity of the aqueous solutions or the vapor pressure of the ADAMs have to be evaluated. It is worthwhile to invest this effort and to pursue on this path towards tailor-made amines. More generally, the present work shows that understanding the influence of the structure of an amine on the speciation of CO_2 -containing species is the key step in establishing relationships between the structure and the application properties of the aqueous solutions of amines.

7. Acknowledgement

We gratefully acknowledge the financial support of the present work by the Federal Ministry of Economic Affairs and Energy of the Federal Republic of Germany (grant no. 03ET1098) and by Evonik and thyssenkrupp.

8. Supporting Information

- \bullet Elucidation of $\rm CO_2\text{-}containing}$ species in $\rm CO_2\text{-}loaded}$ aqueous solutions of EvA07 and EvA21 by NMR spectroscopy
- \bullet Formation of alkylcarbonates in $\mathrm{CO}_2\text{-loaded}$ aqueous solutions of ethanol
- \bullet Numerical experimental data

9. Tables

Table 1: BM-values of the EvAs calculated from Equation (3) with pK-values at 40 °C (cf. Figure 2).

	BM-value
EvA01	11.5
EvA02	8.5
EvA03	10.6
EvA04	9.1
EvA05	8.5
$\text{EvA}06^a$	7.9
EvA07	10.1
$\text{EvA}09^a$	6.8
EvA10	8.3
EvA14	9.5
EvA17	9.2
$\text{EvA}19^a$	6.9
$\text{EvA}21^a$	8.1
$\text{EvA}24^a$	8.3
EvA25	9.7
EvA26	9.2
$\text{EvA}27^a$	8.0
$\text{EvA}31^a$	8.5
$\text{EvA}32^a$	6.9
EvA34	11.2
EvA36	11.6

 $[^]a\mathrm{EvAs}$ that contain oxygen atoms

Table 2: Equilibrium $\rm CO_2$ -loadings of EvA02 and EvA05 at three selected conditions C1, C2, and C3.

	t	p_{CO_2}	$\tilde{w}_{ ext{EvA}}^0$	EvA02	EvA05
	/ °C		/ g/g	$\tilde{X}_{\mathrm{CO}_2}$	/ g/g
$C1^a$	20	2.00	0.10	0.41	0.32
$C2^b$	40	0.14	0.05	0.39	0.32
$C3^b$	100	0.14	0.05	0.16	0.17

t: temperature with the expanded uncertainty U(t) = 1 °C, p_{CO_2} : partial pressure of CO_2 with the relative standard uncertainty $u_r(p_{\text{CO}_2}) = 0.035$, \tilde{w}_{EvA}^0 : mass fraction of EvA in the unloaded solvent with the relative expanded uncertainty $U_r(\tilde{w}_{\text{EvA}}^0) = 0.001$ (0.99 level of confidence), \tilde{X}_{CO_2} : equilibrium CO_2 -loading with the relative standard uncertainty $u_r(\tilde{X}_{\text{CO}_2}) = 0.05$. ^aresults from the present work, ^bresuls from a previous work [47].

10. Figures



Figure 1: Scheme of the route that we have followed in the present study for establishing structure-property relationships. 1st step: establishing relationships between the chemical structure and the speciation. 2nd step: relate the studied speciation to measured application properties of the solvent. ^afrom experiments of the present work, ^bfrom experiments of a previously performed screening [47].

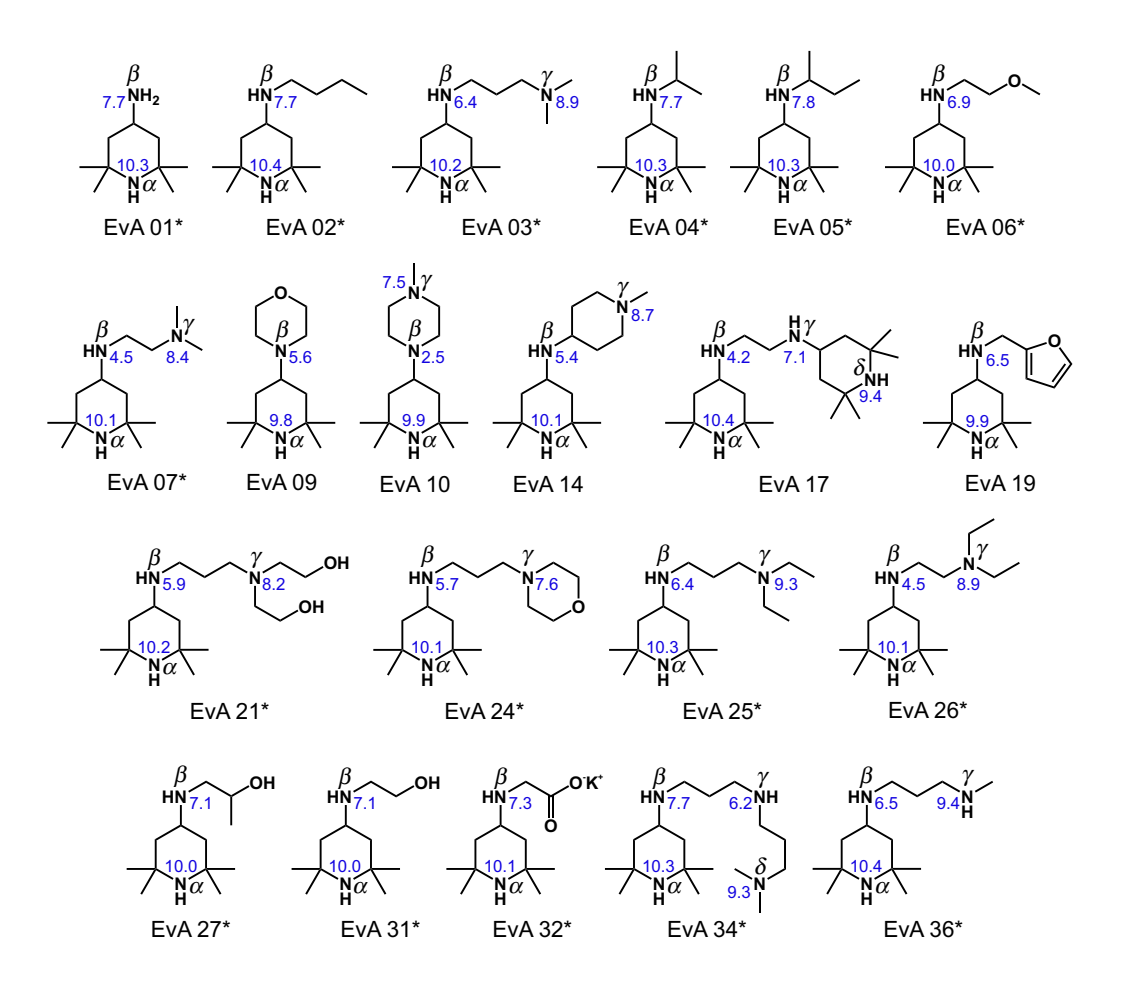


Figure 2: Chemical structures and designations of the EvAs of the present work. Asterisks (*) mark the EvAs that were investigated with NMR spectroscopy. Greek letters are used for designating the amino groups. pK-values of the amino groups at 40 °C are given as numbers shown in blue [47].

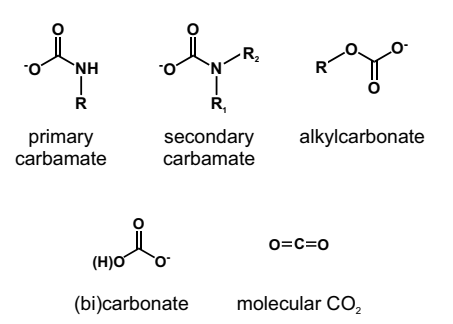


Figure 3: Chemical structures of the observed CO_2 -containing species of the present work.

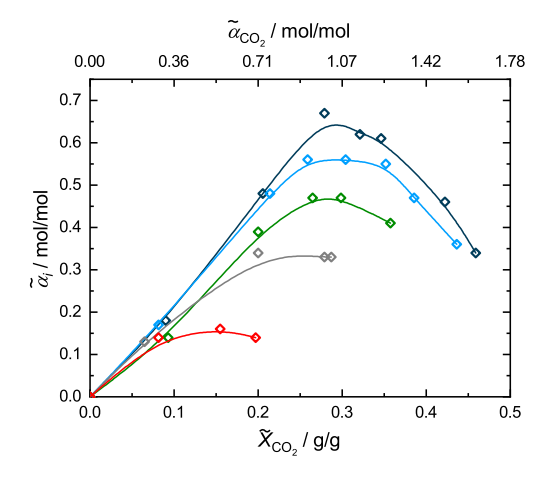


Figure 4: Group A: Speciation in CO_2 -loaded aqueous solutions of EvA01. Results from NMR experiments of the present work. \diamondsuit : β -carbamate, black: 20 °C, blue: 40 °C, green: 60 °C, gray: 80 °C, red: 100 °C. Lines are guides to the eye.

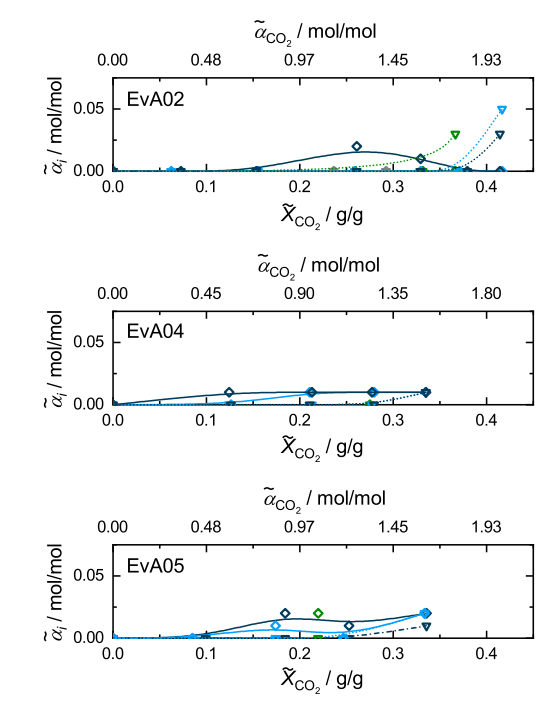


Figure 5: Group B: Speciation in CO_2 -loaded aqueous solutions of EvA02, EvA04, and EvA05. Results from NMR experiments of the present work. \diamond : β -carbamate, ∇ : molecular CO_2 , black: 20 °C, blue: 40 °C, green: 60 °C, gray: 80 °C. Lines are guides to the eye.

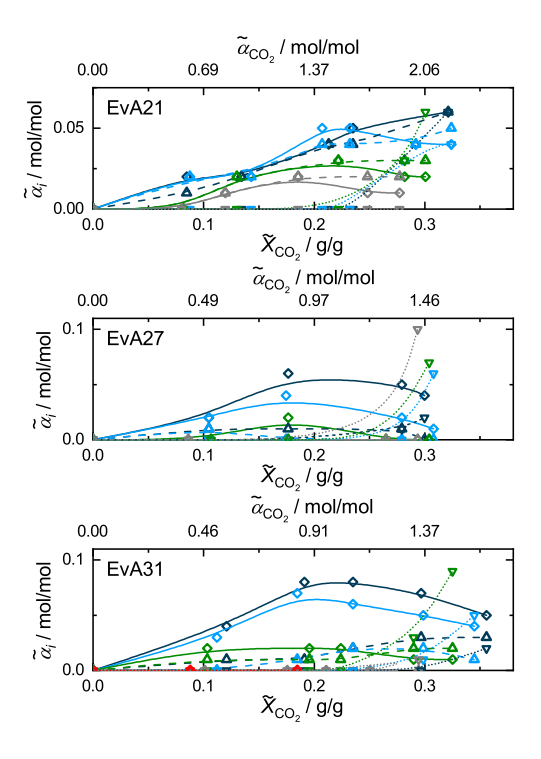


Figure 6: Group C: Speciation in CO_2 -loaded aqueous solutions of EvA21, EvA27, and EvA31. Results from NMR experiments of the present work. \diamondsuit : β -carbamate, \triangle : alkylcarbonate, ∇ : molecular CO_2 , black: 20 °C, blue: 40 °C, green: 60 °C, gray: 80 °C, red: 100 °C. Lines are guides to the eye.

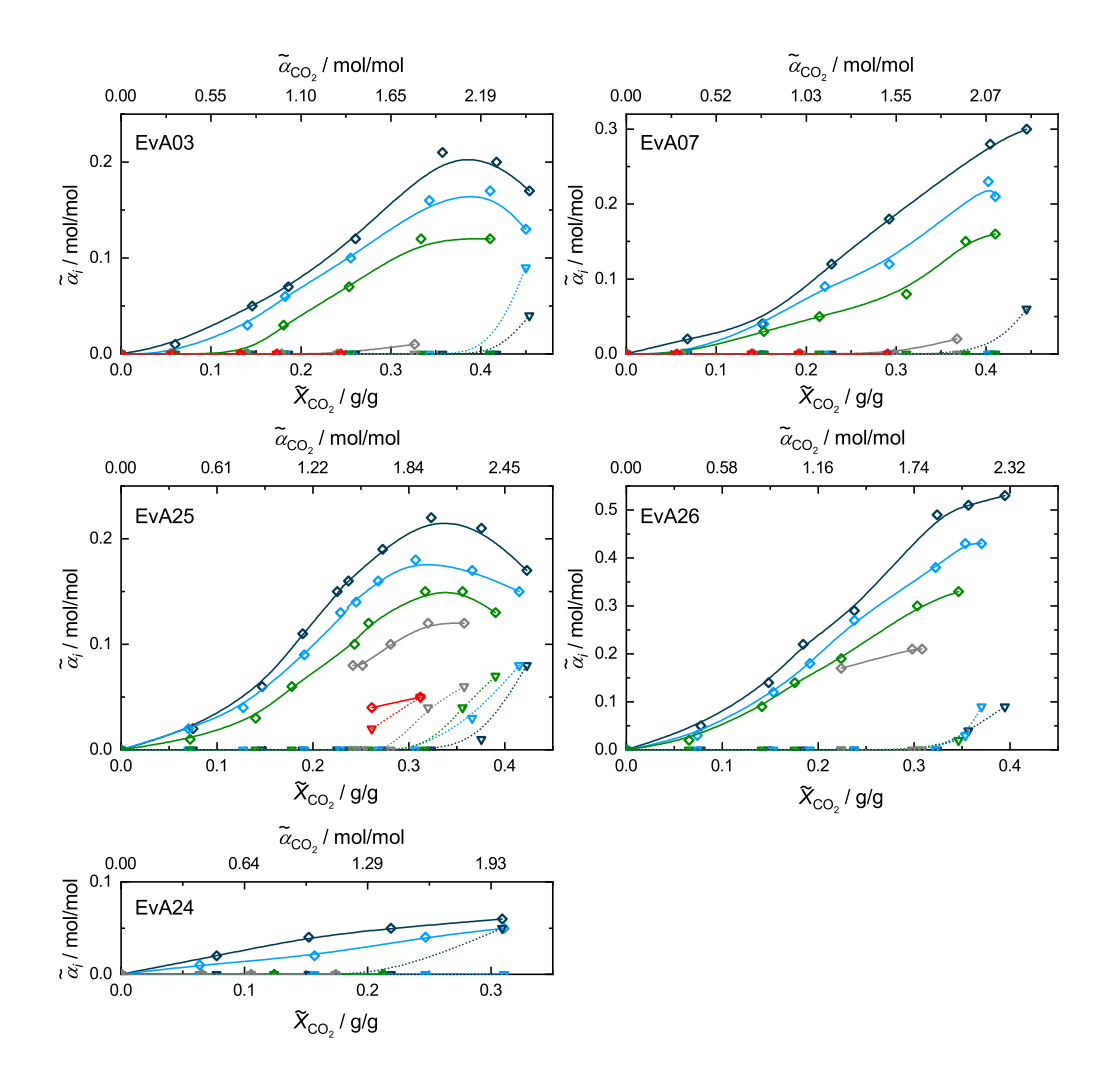


Figure 7: Group D: Speciation in CO_2 -loaded aqueous solutions of EvA03, EvA07, EvA24, EvA25, and EvA26. Results from NMR experiments of the present work. \diamondsuit : β -carbamate, \triangledown : molecular CO_2 , black: 20 °C, blue: 40 °C, green: 60 °C, gray: 80 °C, red: 100 °C. Lines are guides to the eye.

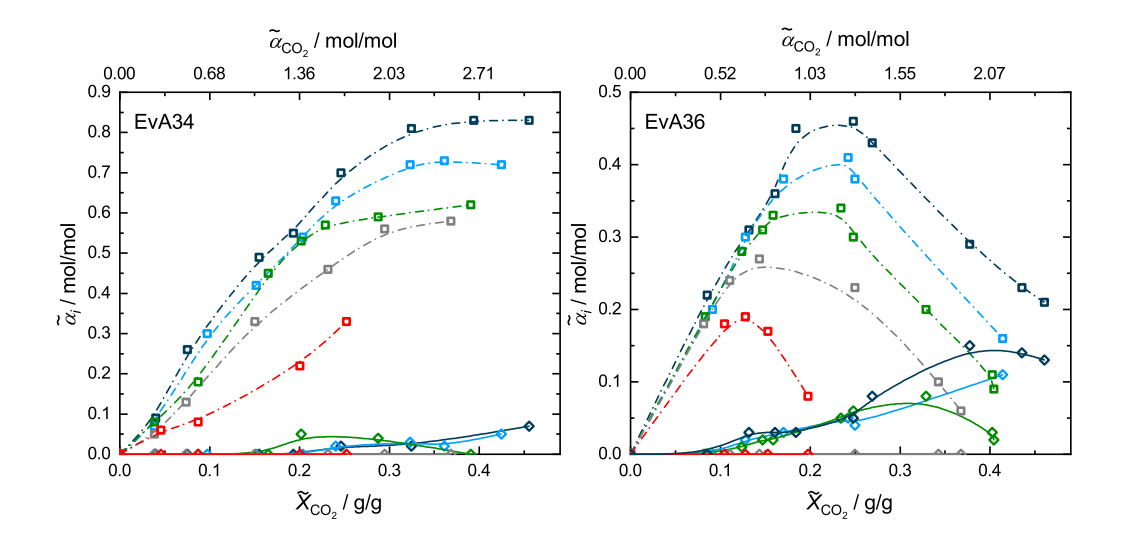


Figure 8: Group E: Speciation in CO₂-loaded aqueous solutions of EvA34 and EvA36. Results from NMR experiments of the present work. \diamondsuit : β -carbamate, \Box : γ -carbamate, black: 20 °C, blue: 40 °C, green: 60 °C, gray: 80 °C, red: 100 °C. Lines are guides to the eye.

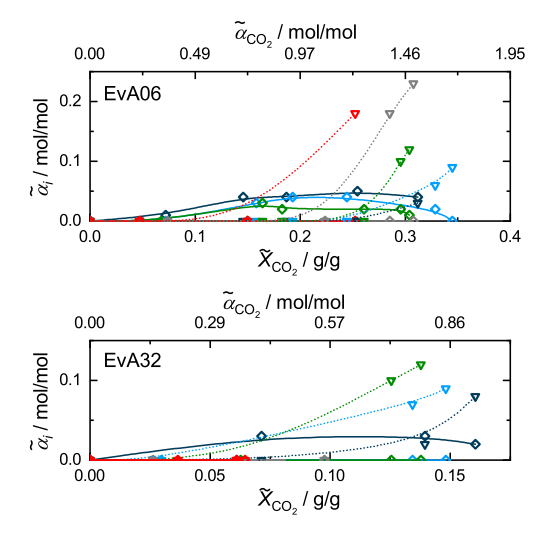


Figure 9: Group F: Speciation in CO₂-loaded aqueous solutions of EvA06 and EvA32. Results from NMR experiments of the present work. \diamondsuit : β -carbamate, ∇ : molecular CO₂, black: 20 °C, blue: 40 °C, green: 60 °C, gray: 80 °C, red: 100 °C. Lines are guides to the eye.

$$R_{\parallel}$$
 R_{\parallel} R_{\parallel

Figure 10: Reaction scheme for the formation of a carbamate zwitterion between β -carbamate and γ -amino group in aqueous solutions of EvA, exemplarily shown for EvA07. See text for description.

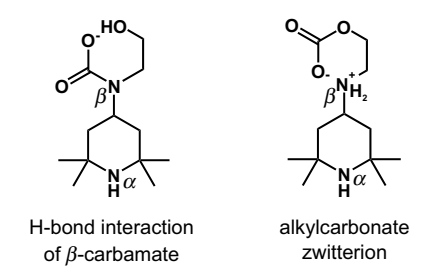


Figure 11: Chemical structures of the stabilizing ring structures in hydroxy group-containing EvAs, exemplarily shown for EvA31.

steric hindrance	primary amine NH ₂ R	secondary amine R, R, R, H, R,
unhindered	3 R = H 2 R = H	3 R ₁ = H & 3 R ₇ = H 2 R ₁ = H & 3 R ₇ = H 2 R ₁ = H & 2 R ₇ = H
single	1 R = H	1 R ₁ = H & 3 R _r = H 1 R ₁ = H & 2 R _r = H
double	0 R = H	1 R _i = H & 1 R _r = H 0 R _i = H & 3 R _r = H 0 R _i = H & 2 R _r = H
triple	-	$0 R_{i} = H \& 1 R_{r} = H$
quadruple	-	0 R ₁ = H & 0 R _r = H

Figure 12: Definition of the degrees of steric hindrance used in the present work.

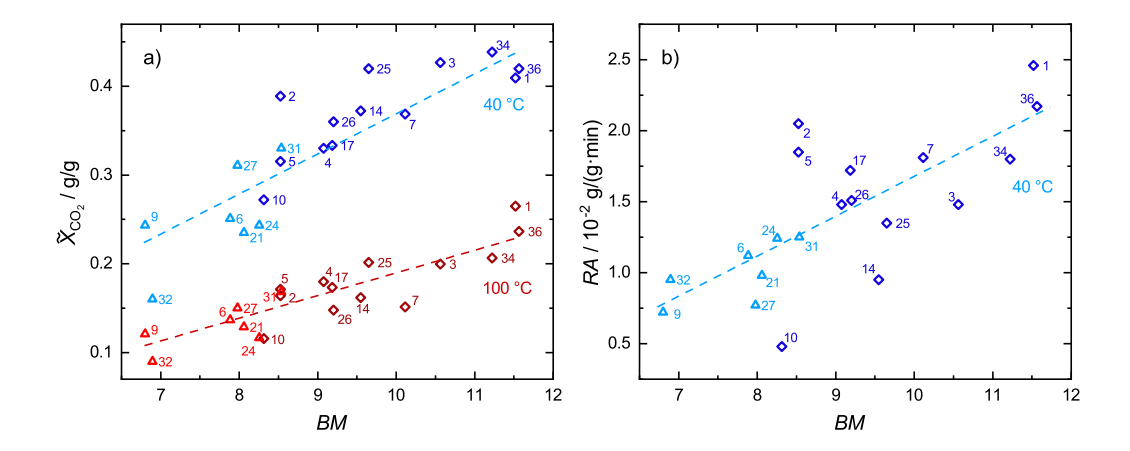


Figure 13: Equilibrium CO_2 -loading $\tilde{X}_{\mathrm{CO}_2}$ and initial rate of absorption of CO_2 RA from [47] as a function of the mass-related basicity BM-value (cf. Section 4.1). Numbers indicate the EvA-number. blue: 40 °C, red: 100 °C, \triangle : EvAs that contain oxygen atoms, \diamondsuit : EvAs that do not contain oxygen atoms, --: linear trend of all isothermal data.

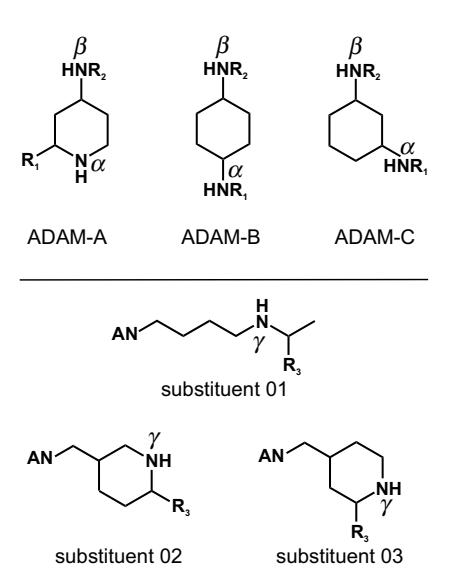


Figure 14: Basic chemical structures of the Advanced Designed Amines (ADAMs) and a selection of substituents. The positions marked with R_1 , R_2 , and R_3 are intended for modifications with varying substituents (see text). AN is where the shown substituents are covalently bound to the β -amino group of the ADAM.

References

- A. L. Kohl, R. B. Nielsen, Gas Purification, 5th Edition, Gulf Publishing Company, Houston, 1997. doi:10.1016/B978-0-88415-220-0.X5000-9.
- [2] Hydrocarbon Processing Industry, 2012 Gas Processes Handbook, Gulf Publishing Company, Houston, 2012.
- [3] B. Metz, O. Davidson, H. de Coninck, M. Loos, L. Meyer, IPCC special report on carbon dioxide capture and storage, IPCC, Cambridge, 2005.
- [4] T. E. Rufford, S. Smart, G. Watson, B. F. Graham, J. Boxall, J. C. Diniz da Costa, E. F. May, The removal of co2 and n2 from natural gas. a review of conventional and emerging process technologies, J. Pet. Sci. Eng. 94-95 (2012) 123–154. doi:10.1016/j.petrol.2012.06.016.
- [5] B. Suresh, R. Gubler, H. Xiaoxiong, Y. Yamaguchi, Chemical Economics Handbook Hydrogen, IHS Markit, Englewood, 2015.
- [6] T. Kuramochi, A. Ramírez, W. Turkenburg, A. Faaij, Comparative assessment of co2 capture technologies for carbon-intensive industrial processes, Prog. Energy Combust. Sci. 38 (2012) 87–112. doi:10.1016/j.pecs.2011.05.001.
- [7] J. Rolker, M. Seiler, New energy-efficient absorbents for the co2 separation from natural gas, syngas and flue gas, Adv. Chem. Eng. Sci. 1 (2011) 280–288. doi:10.4236/aces.2011.14039.
- [8] Ö. Yildirim, A. A. Kiss, N. Hüser, K. Leßmann, E. Y. Kenig, Reactive absorption in chemical process industry: A review on current activities, Chem. Eng. J. 213 (2012) 371–391. doi:10.1016/j.cej.2012.09.121.
- [9] P. Singh, J. P. M. Niederer, G. F. Versteeg, Structure and activity relationships for amine based co2 absorbents i, Int. J. Greenhouse Gas Control 1 (2007) 5–10. doi:10.1016/S1750-5836(07)00015-1.
- [10] P. Singh, G. F. Versteeg, Structure and activity relationships for co2 regeneration from aqueous amine-based absorbents, Process Saf. Environ. Prot. 86 (2008) 347– 359. doi:10.1016/j.psep.2008.03.005.
- [11] P. Singh, D. Brilman, M. Groeneveld, Solubility of co2 in aqueous solution of newly developed absorbents, Energy Procedia 1 (2009) 1257–1264. doi:10.1016/j.egypro.2009.01.165.

- [12] P. Singh, J. P. M. Niederer, G. F. Versteeg, Structure and activity relationships for amine-based co2 absorbents ii, Chem. Eng. Res. Des. 87 (2009) 135–144. doi:10.1016/j.cherd.2008.07.014.
- [13] P. Singh, D. W. F. Brilman, M. J. Groeneveld, Evaluation of co2 solubility in potential aqueous amine-based solvents at low co2 partial pressure, Int. J. Greenhouse Gas Control 5 (2011) 61–68. doi:10.1016/j.ijggc.2010.06.009.
- [14] Z. Wang, M. Fang, Y. Pan, S. Yan, Z. Luo, Amine-based absorbents selection for co2 membrane vacuum regeneration technology by combined absorption—desorption analysis, Chem. Eng. Sci. 93 (2013) 238–249. doi:10.1016/j.ces.2013.01.057.
- [15] F. A. Chowdhury, H. Okabe, S. Shimizu, M. Onoda, Y. Fujioka, Development of novel tertiary amine absorbents for co2 capture, Energy Procedia 1 (2009) 1241– 1248. doi:10.1016/j.egypro.2009.01.163.
- [16] F. A. Chowdhury, H. Okabe, H. Yamada, M. Onoda, Y. Fujioka, Synthesis and selection of hindered new amine absorbents for co2 capture, Energy Procedia 4 (2011) 201–208. doi:10.1016/j.egypro.2011.01.042.
- [17] C. Perinu, B. Arstad, K.-J. Jens, Nmr spectroscopy applied to amine—co2—h2o systems relevant for post-combustion co2 capture. a review, Int. J. Greenhouse Gas Control 20 (2014) 230—243. doi:10.1016/j.ijggc.2013.10.029.
- [18] R. Zhang, Q. Yang, Z. Liang, G. Puxty, R. J. Mulder, J. E. Cosgriff, H. Yu, X. Yang, Y. Xue, Toward efficient co2 capture solvent design by analyzing the effect of chain lengths and amino types to the absorption capacity, bi-carbonate/carbamate, and cyclic capacity, Energy Fuels 31 (2017) 11099–11108. doi:10.1021/acs.energyfuels.7b01951.
- [19] C. Perinu, I. M. Bernhardsen, D. D. D. Pinto, H. K. Knuutila, K. J. Jens, Aqueous mapa, deea, and their blend as co2 absorbents. interrelationship between nmr speciation, ph, and heat of absorption data, Ind. Eng. Chem. Res. 58 (2019) 9781–9794. doi:10.1021/acs.iecr.9b01437.
- [20] D. Fernandes, W. Conway, R. Burns, G. Lawrance, M. Maeder, G. Puxty, Investigations of primary and secondary amine carbamate stability by 1h nmr spectroscopy for post combustion capture of carbon dioxide, J. Chem. Thermodyn. 54 (2012) 183–191. doi:10.1016/j.jct.2012.03.030.

- [21] E. F. da Silva, H. F. Svendsen, Study of the carbamate stability of amines using ab initio methods and free-energy perturbations, Ind. Eng. Chem. Res. 45 (2006) 2497–2504. doi:10.1021/ie050501z.
- [22] K. Goto, H. Okabe, F. A. Chowdhury, S. Shimizu, Y. Fujioka, M. Onoda, Development of novel absorbents for co2 capture from blast furnace gas, Int. J. Greenhouse Gas Control 5 (2011) 1214–1219. doi:10.1016/j.ijggc.2011.06.006.
- [23] G. Sartori, W. S. Ho, D. W. Savage, G. R. Chludzinski, S. Wlechert, Sterically-hindered amines for acid-gas absorption, Sep. Purif. Methods 16 (1987) 171–200. doi:10.1080/03602548708058543.
- [24] W. Conway, X. Wang, D. Fernandes, R. Burns, G. Lawrance, G. Puxty, M. Maeder, Toward the understanding of chemical absorption processes for post-combustion capture of carbon dioxide. electronic and steric considerations from the kinetics of reactions of co2(aq) with sterically hindered amines, Environ. Sci. Technol. 47 (2013) 1163–1169. doi:10.1021/es3025885.
- [25] N. McCann, D. Phan, D. Fernandes, M. Maeder, A systematic investigation of carbamate stability constants by 1h nmr, Int. J. Greenhouse Gas Control 5 (2011) 396–400. doi:10.1016/j.ijggc.2010.01.008.
- [26] Y. E. Kim, S. J. Moon, Y. I. Yoon, S. K. Jeong, K. T. Park, S. T. Bae, S. C. Nam, Heat of absorption and absorption capacity of co2 in aqueous solutions of amine containing multiple amino groups, Sep. Purif. Technol. 122 (2014) 112–118. doi:10.1016/j.seppur.2013.10.030.
- [27] R. J. Hook, An investigation of some sterically hindered amines as potential carbon dioxide scrubbing compounds, Ind. Eng. Chem. Res. 36 (1997) 1779–1790. doi:10.1021/ie9605589.
- [28] C. Perinu, I. M. Bernhardsen, D. D. D. Pinto, H. K. Knuutila, K.-J. Jens, Nmr speciation of aqueous mapa, tertiary amines, and their blends in the presence of co2. influence of pka and reaction mechanisms, Ind. Eng. Chem. Res. 57 (2018) 1337–1349. doi:10.1021/acs.iecr.7b03795.
- [29] Q. Yang, G. Puxty, S. James, M. Bown, P. Feron, W. Conway, Toward intelligent co2 capture solvent design through experimental solvent development and amine synthesis, Energy Fuels 30 (2016) 7503-7510. doi:10.1021/acs.energyfuels.6b00875.
- [30] E. Kessler, L. Ninni, T. Breug-Nissen, B. Willy, R. Schneider, M. Irfan, J. Rolker, E. von Harbou, H. Hasse, Physicochemical properties of the sys-

- tem n,n-dimethyl-dipropylene-diamino-triacetonediamine (eva34), water, and carbon dioxide for reactive absorption, J. Chem. Eng. Data 64 (2019) 2368–2379. doi:10.1021/acs.jced.8b01174.
- [31] W. Böttinger, M. Maiwald, H. Hasse, Online nmr spectroscopic study of species distribution in mea-h2o-co2 and dea-h2o-co2, Fluid Phase Equilib. 263 (2008) 131– 143. doi:10.1016/j.fluid.2007.09.017.
- [32] W. Böttinger, M. Maiwald, H. Hasse, Online nmr spectroscopic study of species distribution in mdea-h2o-co2 and mdea-pip-h2o-co2, Ind. Eng. Chem. Res. 47 (2008) 7917–7926. doi:10.1021/ie800914m.
- [33] R. Behrens, E. von Harbou, W. R. Thiel, W. Böttinger, T. Ingram, G. Sieder, H. Hasse, Monoalkylcarbonate formation in methyldiethanolamine-h2o-co2, Ind. Eng. Chem. Res. 56 (2017) 9006–9015. doi:10.1021/acs.iecr.7b01937.
- [34] R. Behrens, E. Kessler, K. Münnemann, H. Hasse, E. von Harbou, Monoalkylcarbonate formation in the system monoethanolamine–water–carbon dioxide, Fluid Phase Equilib. 486 (2019) 98–105. doi:10.1016/j.fluid.2018.12.031.
- [35] M. Vogt, C. Pasel, D. Bathen, Characterisation of co2 absorption in various solvents for pcc applications by raman spectroscopy, Energy Procedia 4 (2011) 1520–1525. doi:10.1016/j.egypro.2011.02.020.
- [36] P. G. L. Samarakoon, N. H. Andersen, C. Perinu, K.-J. Jens, Equilibria of mea, dea and amp with bicarbonate and carbamate. a raman study, Energy Procedia 37 (2013) 2002–2010. doi:10.1016/j.egypro.2013.06.080.
- [37] V. Souchon, M. d. O. Aleixo, O. Delpoux, C. Sagnard, P. Mougin, A. Wender, L. Raynal, In situ determination of species distribution in alkanolamineh2o - co2 systems by raman spectroscopy, Energy Procedia 4 (2011) 554–561. doi:10.1016/j.egypro.2011.01.088.
- [38] P. Jackson, K. Robinson, G. Puxty, M. Attalla, In situ fourier transform-infrared (ftir) analysis of carbon dioxide absorption and desorption in amine solutions, Energy Procedia 1 (2009) 985–994. doi:10.1016/j.egypro.2009.01.131.
- [39] P. Muchan, C. Saiwan, J. Narku-Tetteh, R. Idem, T. Supap, P. Tontiwachwuthikul, Screening tests of aqueous alkanolamine solutions based on primary, secondary, and tertiary structure for blended aqueous amine solution selection in post combustion co2 capture, Chem. Eng. Sci. 170 (2017) 574–582. doi:10.1016/j.ces.2017.02.031.

- [40] D. Fernandes, W. Conway, X. Wang, R. Burns, G. Lawrance, M. Maeder, G. Puxty, Protonation constants and thermodynamic properties of amines for post combustion capture of co2, J. Chem. Thermodyn. 51 (2012) 97–102. doi:10.1016/j.jct.2012.02.031.
- [41] F. Khalili, A. Henni, A. L. L. East, pka values of some piperazines at (298, 303, 313, and 323 k), J. Chem. Eng. Data 54 (2009) 2914–2917. doi:10.1021/je900005c.
- [42] A. V. Rayer, K. Z. Sumon, L. Jaffari, A. Henni, Dissociation constants (pka) of tertiary and cyclic amines. structural and temperature dependences, J. Chem. Eng. Data 59 (2014) 3805–3813. doi:10.1021/je500680q.
- [43] Y. Mergler, R. R.-v. Gurp, P. Brasser, M. d. Koning, E. Goetheer, Solvents for co2 capture. structure-activity relationships combined with vapour-liquid-equilibrium measurements, Energy Procedia 4 (2011) 259–266. doi:10.1016/j.egypro.2011.01.050.
- [44] N. El Hadri, D. V. Quang, E. L. V. Goetheer, M. R. M. A. Zahra, Aqueous amine solution characterization for post-combustion co2 capture process, Appl. Energy 185 (2017) 1433–1449. doi:10.1016/j.apenergy.2016.03.043.
- [45] G. Puxty, R. Rowland, A. Allport, Q. Yang, M. Bown, R. Burns, M. Maeder, M. Attalla, Carbon dioxide postcombustion capture. a novel screening study of the carbon dioxide absorption performance of 76 amines, Environ. Sci. Technol. 43 (2009) 6427–6433. doi:10.1021/es901376a.
- [46] S. Singto, T. Supap, R. Idem, P. Tontiwachwuthikul, S. Tantayanon, M. J. Al-Marri, A. Benamor, Synthesis of new amines for enhanced carbon dioxide (co2) capture performance, the effect of chemical structure on equilibrium solubility, cyclic capacity, kinetics of absorption and regeneration, and heats of absorption and regeneration, Sep. Purif. Technol. 167 (2016) 97–107. doi:10.1016/j.seppur.2016.05.002.
- [47] E. Kessler, L. Ninni, D. Vasiliu, A. Yazdani, B. Willy, R. Schneider, M. Irfan, J. Rolker, E. von Harbou, H. Hasse, Triacetone-amine derivatives (evas) for co2absorption from process gases, Int. J. Greenhouse Gas Control 95 (2020) 102932. doi:10.1016/j.ijggc.2019.102932.
- [48] Á. Pérez-Salado Kamps, G. Maurer, Dissociation constant of n-methyldiethanolamine in aqueous solution at temperatures from 278 k to 368 k, J. Chem. Eng. Data 41 (6) (1996) 1505–1513. doi:10.1021/je960141.
- [49] D. Vasiliu, A. Yazdani, N. McCann, M. Irfan, R. Schneider, J. Rolker, G. Maurer, E. von Harbou, H. Hasse, Thermodynamic study of a complex system for carbon

- capture: Butyltriacetonediamine + water + carbon dioxide, J. Chem. Eng. Data 61 (2016) 3814-3826. doi:10.1021/acs.jced.6b00451.
- [50] E. Kessler, L. Ninni, B. Willy, R. Schneider, M. Irfan, J. Rolker, E. von Harbou, H. Hasse, Structure-property relationships for new amines for reactive co2 absorption, Chem. Eng. Trans. 69 (2018) 109–114. doi:10.3303/CET1869019.
- [51] K. Minke, B. Willy, Us patent 20180009734: An n-substituted triacetonediamine compound is produced by reacting 4-amino-2,2,6,6-tetramethylpiperidine or a derivative thereof with a carbonyl compound in a reductive amination (2018).
- [52] S. G. Warren, P. Wyatt, Organic synthesis. The disconnection approach / Stuart Warren and Paul Wyatt, 2nd Edition, Wiley-Blackwell, Oxford, 2008.
- [53] D. D. Perrin, Dissociation Constants of Organic Bases in Aqueous Solution, Butterworths, London, 1965.
- [54] M. Nitta, M. Hirose, T. Abe, Y. Furukawa, H. Sato, Y. Yamanaka, 13c-nmr spectroscopic study on chemical species in piperazine-amine-co2-h2o system before and after heating, Energy Procedia 37 (2013) 869–876. doi:10.1016/j.egypro.2013.05.179.
- [55] M. M. Sharma, Kinetics of reactions of carbonyl sulphide and carbon dioxide with amines and catalysis by brönsted bases of the hydrolysis of cos, Trans. Faraday Soc. 61 (1965) 681–688. doi:10.1039/TF9656100681.
- [56] J. R. Lane, S. D. Schrøder, G. C. Saunders, H. G. Kjaergaard, Intramolecular hydrogen bonding in substituted aminoalcohols, J. Phys. Chem. A 120 (2016) 6371–6378. doi:10.1021/acs.jpca.6b05898.
- [57] D. L. Thomsen, J. L. Axson, S. D. Schrøder, J. R. Lane, V. Vaida, H. G. Kjaergaard, Intramolecular interactions in 2-aminoethanol and 3-aminopropanol, J. Phys. Chem. A 117 (2013) 10260–10273. doi:10.1021/jp405512y.
- [58] G. Sartori, D. W. Savage, Sterically hindered amines for carbon dioxide removal from gases, Ind. Eng. Chem. Fund. 22 (1983) 239–249. doi:10.1021/i100010a016.
- [59] M. Wagner, I. von Harbou, J. Kim, I. Ermatchkova, G. Maurer, H. Hasse, Solubility of carbon dioxide in aqueous solutions of monoethanolamine in the low and high gas loading regions, J. Chem. Eng. Data 58 (2013) 883–895. doi:10.1021/je301030z.
- [60] Á. P.-S. Kamps, J. Xia, G. Maurer, Solubility of co2 in (h2o+piperazine) and in (h2o+mdea+piperazine), AIChE J. 49 (2003) 2662-2670. doi:10.1002/aic.690491019.

- [61] B. Burr, L. Lyddon, A comparison of physical solvents for acid gas removal, GPA Annu. Convention Proc. 1 (2008) 1–13.
- [62] C. Perinu, B. Arstad, A. M. Bouzga, K.-J. Jens, 13c and 15n nmr characterization of amine reactivity and solvent effects in co2 capture, J. Phys. Chem. B 118 (2014) 10167–10174. doi:10.1021/jp503421x.
- [63] C. Perinu, B. Arstad, A. M. Bouzga, J. A. Svendsen, K. J. Jens, Nmr-based carbamate decomposition constants of linear primary alkanolamines for co2 capture, Ind. Eng. Chem. Res. 53 (2014) 14571–14578. doi:10.1021/ie5020603.
- [64] I. Kim, K. A. Hoff, E. T. Hessen, T. Haug-Warberg, H. F. Svendsen, Enthalpy of absorption of co2 with alkanolamine solutions predicted from reaction equilibrium constants, Chem. Eng. Sci. 64 (2009) 2027–2038. doi:10.1016/j.ces.2008.12.037.
- [65] H. Svensson, C. Hulteberg, H. T. Karlsson, Heat of absorption of co2 in aqueous solutions of n-methyldiethanolamine and piperazine, Int. J. Greenhouse Gas Control 17 (2013) 89–98. doi:10.1016/j.ijggc.2013.04.021.
- [66] N. McCann, M. Maeder, M. Attalla, Simulation of enthalpy and capacity of co2 absorption by aqueous amine systems, Ind. Eng. Chem. Res. 47 (2008) 2002–2009. doi:10.1021/ie070619a.
- [67] I. von Harbou, Post-combustion carbon capture by reactive absorption using aqueous amine solutions. experiments, modeling, and simulation, Phd, TU Kaiserslautern, Germany (2013).
- [68] E. Sanchez-Fernandez, F. d. M. Mercader, K. Misiak, L. van der Ham, M. Linders, E. Goetheer, New process concepts for co2 capture based on precipitating amino acids, Energy Procedia 37 (2013) 1160–1171. doi:10.1016/j.egypro.2013.05.213.
- [69] S. Ma'mun, I. Kim, Selection and characterization of phase-change solvent for carbon dioxide capture: precipitating system, Energy Procedia 37 (2013) 331–339. doi:10.1016/j.egypro.2013.05.119.
- [70] S. Yan, M. Fang, Z. Wang, Z. Luo, Regeneration performance of co2-rich solvents by using membrane vacuum regeneration technology. relationships between absorbent structure and regeneration efficiency, App. Energy 98 (2012) 357–367. doi:10.1016/j.apenergy.2012.03.055.
- [71] R. Behrens, M. Dyga, G. Sieder, Erik, H. Hasse, Nmr spectroscopic method for studying homogenous liquid phase reaction kinetics in systems used in reactive gas

absorption and application to monoethanolamine–water–carbon dioxide, Chem. Eng. J. 374 (2019) 1127–1137. doi:10.1016/j.cej.2019.05.189.